

# Effect of staggered arrays on cooling characteristics of impinging water jet on a hot steel plate

J. Lee, T. H. Kim, K. H. Do, D-W. Oh, J. M. Park

*Water impinging jet has been widely used in cooling of hot steel plate at steelmaking processes. The effects of staggered arrays on water impinging jet cooling were mainly investigated at fixed jet Reynolds number of 35,000 and nozzle-to-plate distance of 100 mm. The time-and space-resolved heat flux was experimentally measured with different staggered geometric array configurations which are considered to 3D, 4D, 5D, 6D, 8D, and 10D, respectively. The heat flux were measured by a novel experimental technique that has a function of high-temperature heat flux gauge in which is used to measure the heat flux distributions on the hot surface. The qualitative flow visualization showed complex behavior for staggered array configuration, which exhibits a radial flow interaction issuing from adjacent nozzles. The results show that the maximum area-averaged heat flux was observed at  $S/D = 4$ . This was caused by the radial interaction between adjacent jets which affects different boiling heat transfer on a hot steel plate. In this study, the measured heat flux curves are also provided to a benchmark data for designing a new type of accelerated cooling equipment for plate mill.*

**Keywords:** Staggered array - Water jet cooling - Boiling - Hot steel plate

## INTRODUZIONE

Water impinging jet has been an effective method of cooling due to high heat transfer rate in steelmaking processes which include the Runout-table cooling of hot rolled mill, the accelerated cooling of plate mill, and the bar cooling of wire-rod mill [1]. Water impinging jet is well known as the representative cooling method of removing high heat fluxes during cooling of a hot steel plate, so many previous studies have been consecutively conducted in the concept of jet impingement boiling [2].

There were relatively scarce to find out the literature on water cooling/quenching for staggered array of impinging water jet on a steel plate. Pan and Webb (1995) investigated flow and heat transfer characteristics of in-line and staggered array of free-surface water jets in the non-boiling regime. They suggested that the stagnation heat transfer was observed midway between adjacent jets, which were highly attributed to the interjet flow interaction [3]. However, there were no experimental studies on the ef-

fect of staggered arrays of free-surface impinging jets on boiling heat transfer in actual hot steel surface of 900°C. A sort of staggered arrays of water jets has been applied to an accelerated cooling method of hot steel plate in a field of plate mill. The representative staggered arrays of water jet were found in MULPIC(MULTi-Purpose Interrupt Cooling) which was originally developed by VAI since 1980's. This study is motivated by the fact that accelerated cooling processes of plate mill in steelmaking industries require the effects of staggered arrays of free-surface water impinging jet on its cooling/quenching characteristics. In case of plate mill, the water jet cooling/quenching is nominally started from the austenitic temperature of 800°C to the finish cooling temperature of 400°C, which depends on its target metallurgy. So the current study is to provide quantitative local and average heat transfer characteristics of the staggered arrays of free-surface water impinging jet when new types of accelerated cooling process are required to be designed.

**Jungho Lee, Tae Hoon Kim, Kyu Hyung Do, Dong-wook Oh and Jang Min Park**

*Korea Institute of Machinery and Materials  
Daejeon, Korea*

*Paper presented at the Int. Conf. ROLLING 2013, Venice  
10-12 June 2013, organized by AIM*

## EXPERIMENTAL APPARATUS

The experimental apparatus is schematically shown in Fig. 1. The experimental apparatus consists of a constant-temperature water reservoir, a pump, an electromagnetic flow meter, chamber and staggered array jet nozzle, a heating block assembly with a function of high-temperature heat flux gauge, and a data acquisition system.

A constant temperature reservoir is capable of controlling a constant water temperature within  $\pm 0.5^\circ\text{C}$  and composed of a stainless steel tank of 250 liter, an electric heater of 10 kW, and a refrigerator. The cooling water can be delivered by a pump, which is CRN 1-15 model of Grundfos® and has nearly total head of 100 m. The water flow rate was directly measured by an electromagnetic flow meter, which is GF630A/LF600 model of Toshiba® with an accuracy of  $\pm 0.5\%$  reading. During the experiments, the water flow rate was consistently kept at  $0.336\text{ m}^3/\text{hr}$  as determined from an electromagnetic flow meter connected in the flow loop. The corresponding Reynolds number of water impinging jet was 35,000 based on  $T_w = 15^\circ\text{C}$ . Its measurement uncertainty reached 0.8% for the volumetric flow rate measurement and 3.5% for the jet Reynolds number. The overall experimental apparatus was nearly set up based on author's previous work [4].

A water jet impinges vertically downward and strikes a uni-

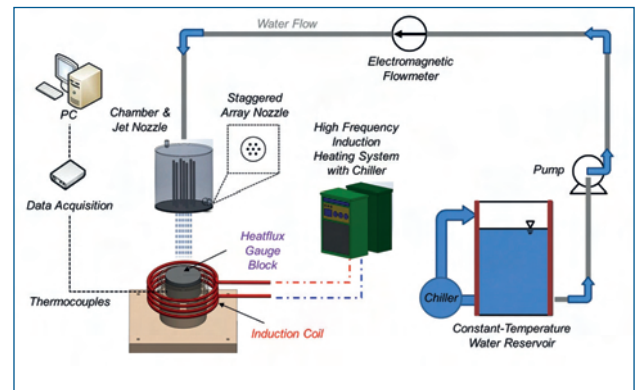


**Fig. 1 - Schematics of the experimental setup for staggered array of water jet.**

*Fig. 1 - Schema dell'impianto sperimentale per getti d'acqua con disposizione sfalsata.*

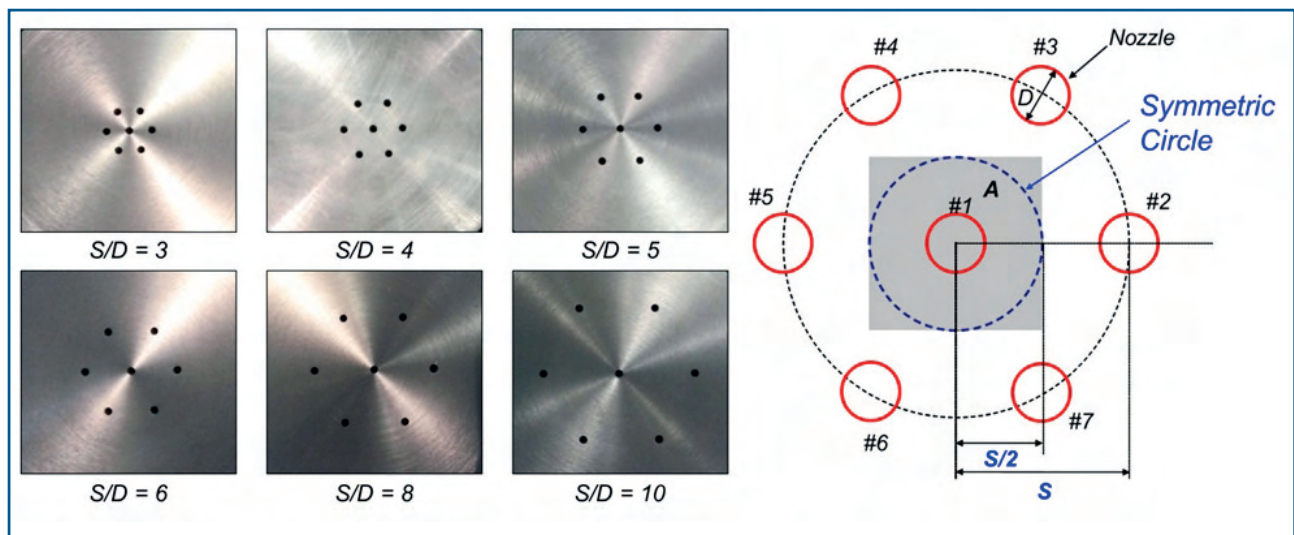


**Fig. 2 - Fabrication and configuration of staggered array nozzles ( $S/D = 3, 4, 5, 6, 8$  and  $10$ ).**

*Fig. 2 - Fabbricazione e configurazione degli ugelli a getti sfalsati ( $S/D = 3, 4, 5, 6, 8$  e  $10$ ).*

formly heated surface on which heat flux measurements are made. The nozzle-to-target spacing was held constant at 100 mm and the cooling water temperature was kept constant at  $15^\circ\text{C}$ . Staggered array jets were issued from a chamber with 7 staggered array nozzles which were made of stainless steel tube of 3 mm inner diameter and 90 mm length. This concept of staggered array nozzle configuration was determined from the accelerating cooling machine of MULPIC (MULTi-Purpose Interrupt Cooling) which is already installed at No. 2 and No. 3 Plate Mill of POSCO, Korea.

As shown in Fig. 1, interchangeable staggered array nozzle were attached at the bottom of the settling chamber, each of which was fabricated with six different staggered-type jet array configuration as shown in Fig. 2. A nozzle diameter of 3 mm was fixed at all of staggered array nozzle. The dimensionless jet-to-jet spacings were  $S/D = 3, 4, 5, 6, 8$  and  $10$ . Qualitative flow visualization was also performed by replacing the top surface of heated test block with a Plexiglas flat plate through which the radial jet flow pattern by the staggered array could be seen and achieved by a high-speed CCD camera. Though meaning of area-avera-

ged heat flux for the staggered array jet is a little complicated, the area-averaged heat flux can be determined by symmetric circle as shown in right-side of Fig. 2. Each area-averaged heat flux was calculated on the half of jet-to-jet spacing ( $S/2$ ), because a flow interaction between adjacent jets is clearly seen along the symmetric circle of which radius is  $S/2$ .

A test assembly as a function of the high-temperature heat flux gauge is shown in Fig. 3. The test assembly consists of the test block, the induction heating system, insulators and the thermocouples, and has a function of heat flux gauge during water cooling/quenching experiments. The water jet impinges vertically onto a heated test block, is made of stainless steel AISI-type 314 which avoids additional heat generation during phase-transformation for most

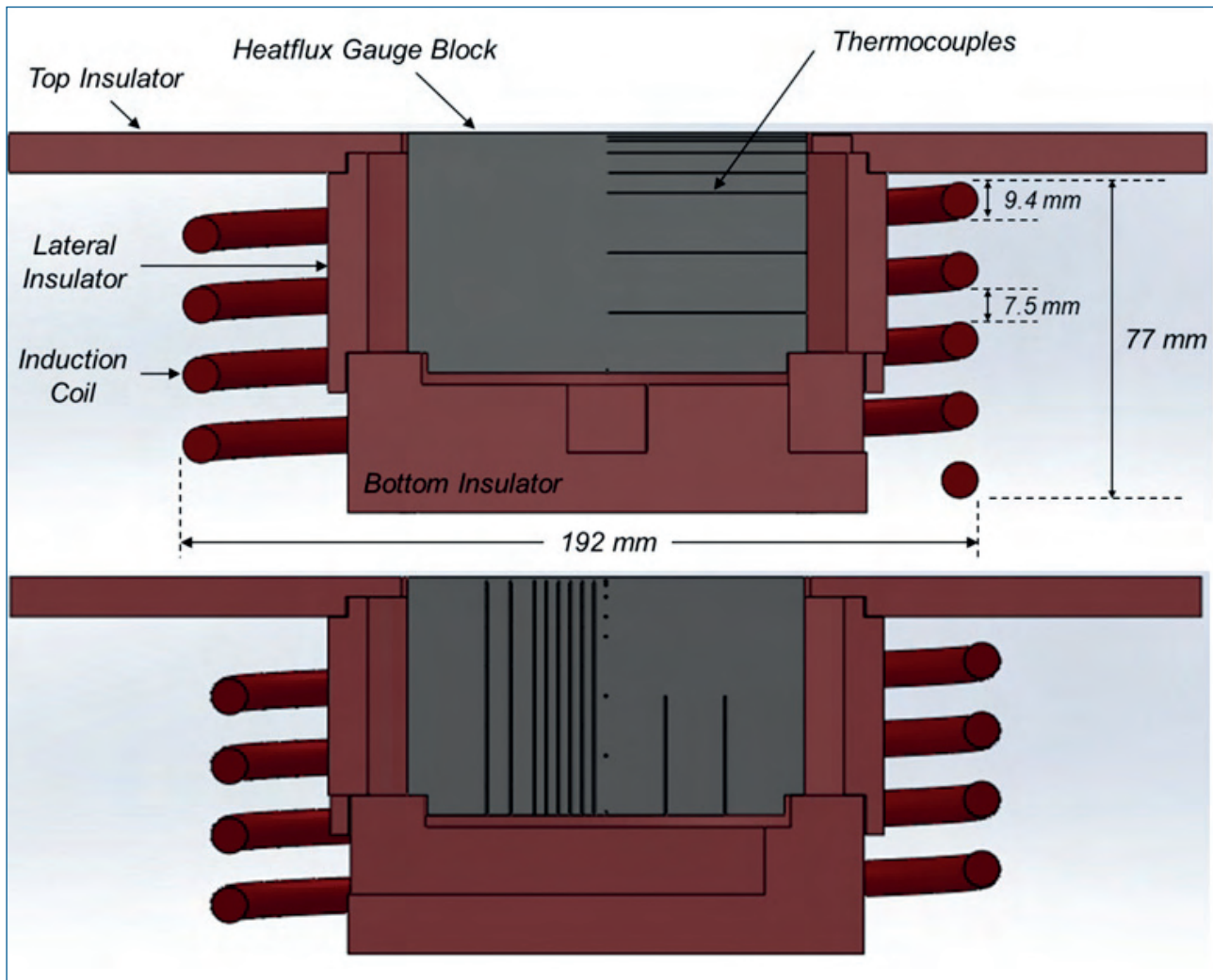


**Fig. 3 - Assemblies of the high-temperature heat flux gauge.**

*Fig. 3 - Configurazione del misuratore del flusso di calore ad alta temperatura*

carbon steels. The test block has a height of 60 mm and a diameter of 100 mm as shown in Fig 4. The test block was designed to reduce geometrically thermal deformation after repeated experiments, because the aspect ratio of the block was almost 1.67, which applied to much less plastic deformation. So the test block can be repeatedly used in the high temperature heating/cooling experiments [4]. The high-frequency induction coil with 9.4 mm tube diameter were installed around the test block and were used to heat the test block electrically up to 1,000°C. 18 K-type (Chromel-Alumel) thermocouples of OMEGA® KMTXL-020G-6 with 0.5 mm thick were installed to measure temperatures at distinct 18 points as shown in Fig. 3. From No. 1 to No. 8 thermocouples are positioned at the center of the block through thickness. No. 1 thermocouple is respectively located at 1 mm apart from the bottom surface; No. 2 thermocouple is located at the bottom quarter of the block (15 mm apart from the bottom surface); No. 3 thermocouple is located at the center of the block (30 mm apart from the bottom surface); No. 4 thermocouple is

also located at the top quarter of the block (15 mm apart from the top surface); No. 5, No. 6, No. 7 and No. 8 thermocouples are respectively located at 10 mm, 5 mm, 2 mm, and 1 mm from the top surface along the centerline of the block.

No. 9 and No. 10 thermocouples are made to check radial temperature change inside the block. No. 8 and 9 thermocouple is installed at the 15 mm and 30 mm from the No. 3 position along the radial direction, respectively. Eight holes of 0.5 mm diameter are drilled using electric discharge machining (EDF) technique from the bottom surface of the test block to a depth of  $59 \pm 0.05$  mm. The thermocouples from No. 11 to No. 18 are located along a radial line. The thermocouples from No. 11 to No. 16 and are spaced 3 mm apart and those from No. 16 to No. 18 are spaced 6 mm apart, respectively. The side and the bottom surface of the test block are also thermally insulated, while heat transfer by water cooling happens from the top surface. This insulation is installed as a combination of ceramic board and Cerakool®.

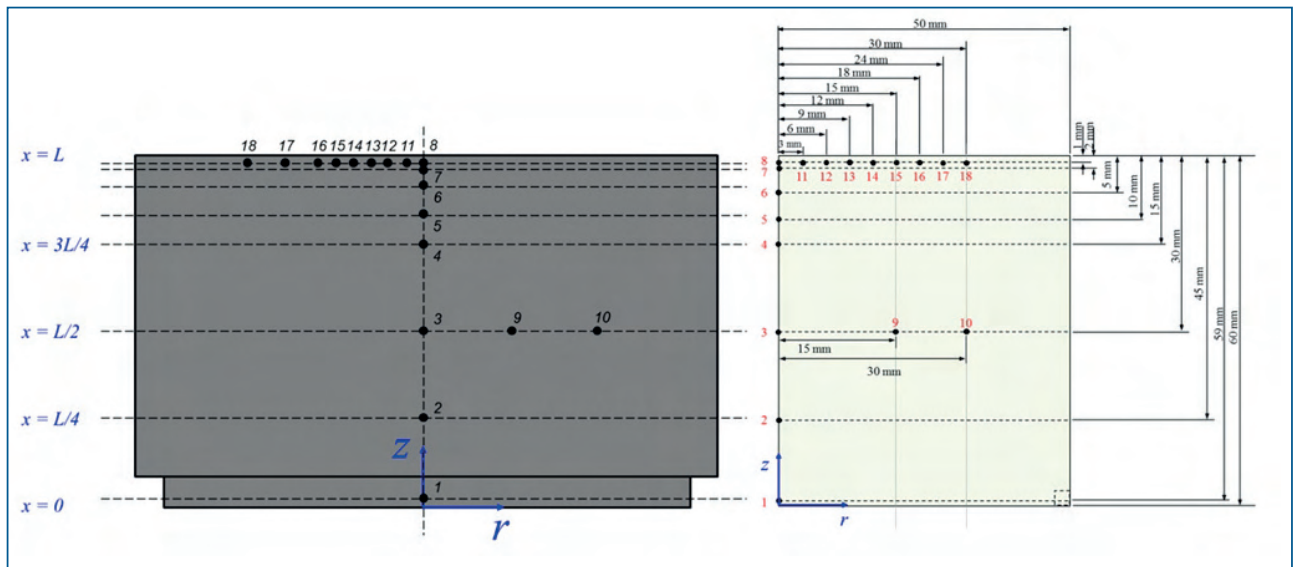


**Fig. 4 - Location of installed 18 thermocouples in the high-temperature heat flux gauge.**

*Fig. 4 - Schema del posizionamento di 18 termocoppie installate nel misuratore del flusso di calore ad alta temperatura*

Before and after experiments, a careful calibration of thermocouples was performed by comparing to the platinum resistance thermometer. The final uncertainty in the measured temperature was  $\pm 0.1^\circ\text{C}$ .

As the temperature of the test block reaches to a saturation of  $950^\circ\text{C}$ , the experiments start to cool/quench the heated surface and the time-dependent temperature histories are recorded by the data acquisition with a sampling of 10 data/sec. FLUKE 2680A data acquisition was employed to achieve and save the measured temperature data within the test block during experiments.

Heat transfer measurement in water impinging jet cooling was investigated by either steady state or transient method. Steady state method depends on a thermal balance between the power input into an appropriate test block and the heat transferred to the water jet, which is highly limited by the maximum attainable power densities. Generally, a power input more than  $10^7$  Watt might be required to keep a test block at a constant temperature, which is clearly unfeasible. Moreover, steady state condition in power controlled system cannot be maintained in the transition boiling regime of the heat flux curve. Due to these limitations, steady state methods are usually confined to heat transfer measurements involving low volumetric flow like as a single droplet. However in transient method, a test block is typically heated to a uniform high temperature and then rapidly cooled by the water impinging jet while the temperatures at one or more inner locations are recorded. As the transient method is the only possible if large heat transfer rates are involved, so this method is adopted at the rapid cooling of water impinging jet [4].

## HEATFLUX DETERMINATION

A two-dimensional inverse heat conduction analysis was employed to estimate the local heat transfer characteristics on the cooled/quenched surface from experimental data which measure the internal temperatures. The formulation of the two-dimensional inverse heat conduction which was used for analysis is based on the trial function method which was developed by Twomey[5] and Beck et al.[6]. The method of the inverse heat conduction analysis is basically to minimize, with respect to the surface heat flux ( $q$ ), the sum of squared function ( $S$ ) can be expressed as

$$S = \sum_{i=0}^N (\mathbf{U}_i - \mathbf{T}_i)^2 \quad (1)$$

Where  $N$ ,  $T$ , and  $U$  are the number of temperature measurement points, measured temperatures, and temperatures estimated by the calculation, respectively. Estimated temperatures ( $U$ ) are obtained from the two-dimensional heat conduction equation as follow:

$$\rho c_p \frac{\partial T}{\partial t} = k \frac{1}{r} \frac{\partial}{\partial r} \left( r \frac{\partial T}{\partial r} \right) + k \frac{\partial^2 T}{\partial z^2} \quad (2)$$

where  $\rho$ ,  $c_p$ , and  $k$  represent density, thermal capacity, and thermal conductivity of the test block, respectively. Temperature dependent thermal properties were also used in the present analysis. A detailed formulation and description of the method was presented in Kwon et al.[7]. Various numerical tests were conducted to validate the formulation, and the results obtained by the present

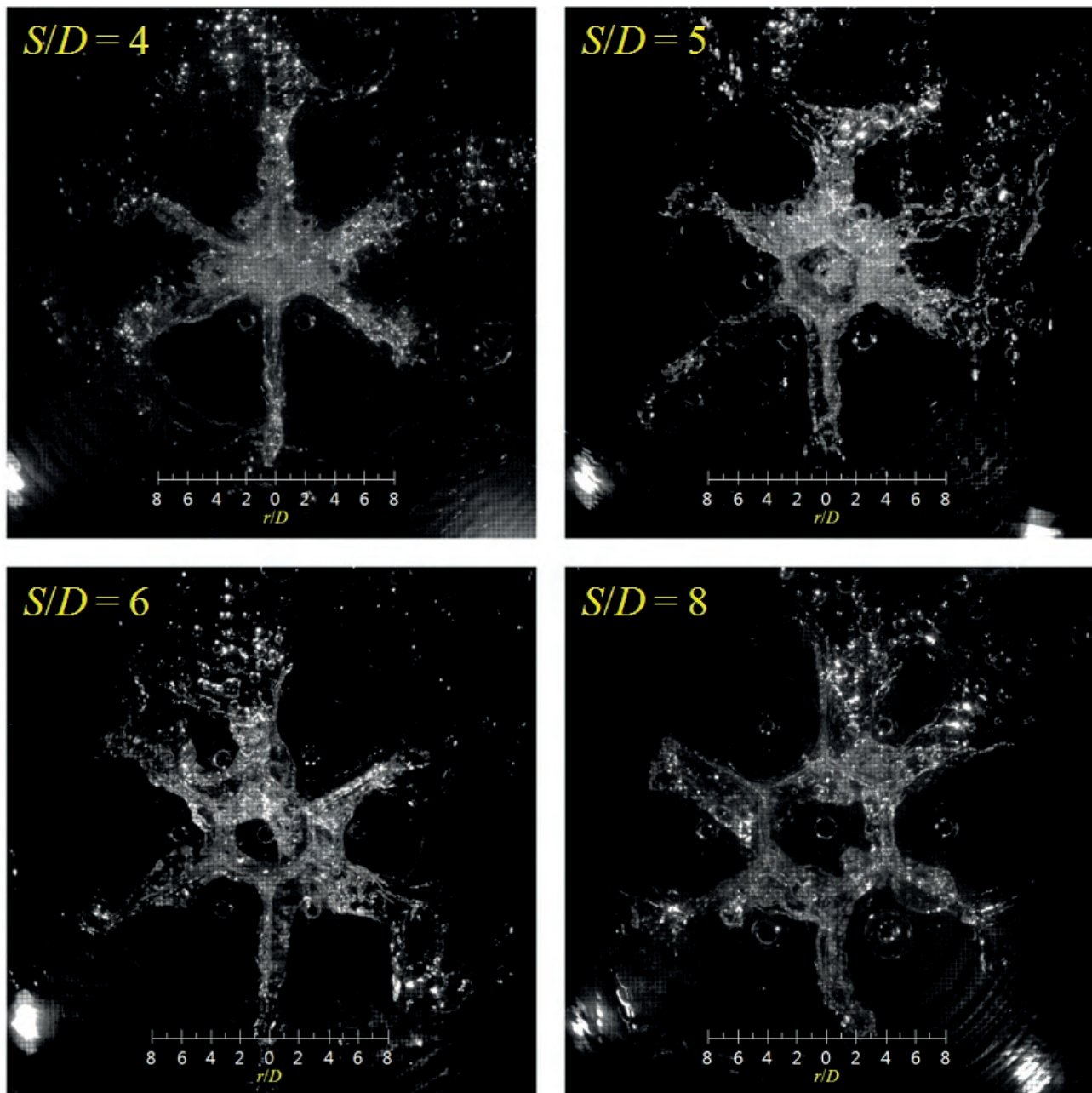


**Fig. 5 - Visualized flow pattern for staggered array of water impinging jet.**

*Fig. 5 - Visualizzazione della configurazione del flusso per i getti d'acqua con disposizione sfalsata.*

method were well matched with the assumed surface heat flux profile.

## RESULTS AND DISCUSSION

The qualitative visualization showed complex flow patterns on the target surface for staggered array configuration, which clearly exhibits a radial flow interaction issuing from adjacent nozzles. Fig. 5 shows typical flow visualized images for staggered array jet of  $S/D = 4, 5, 6,$  and  $8$  at the nozzle-to-target spacing of  $100\text{ mm}$ . At smaller jet-to-jet spacing ( $S/D = 4$ ), a region of superimposed merging

flow between the central jet and surrounding side jets was obviously observed near  $r/D = 2$ . The region merging the central jet and surrounding jet forms a well mixed bubbly two-phase flow observed at near  $r/D = 2$ . This bubbly region might be come from the result of air entrainment between the central jet and the surrounding jets. The spatial extent of the superimposed merging flow around the central jet was reduced for very small jet-to-jet spacing of  $S/D < 2$ . However, at larger jet-to-jet spacing ( $S/D = 6$  and  $8$ ), a superimposed merging flow was not seen at the boundary between the central jet and the surrounding jets. The radial flow between adjacent jets was seen to mutually interact with moderate intensity, which forms a hexagonal

shape in the staggered array jet as shown in larger jet-to-jet spacing of  $S/D = 6$  and  $8$ . The flow visualization results in this study show a nearly identical flow visualized illustration by Pan and Webb [3].

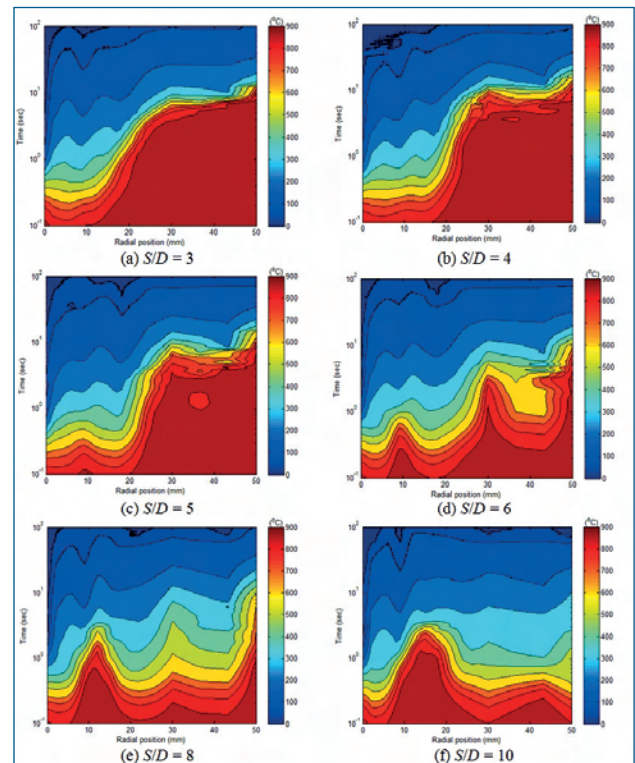
The time-dependent surface temperature contour along the radial direction is shown in Fig. 6. The surface temperatures are seen to change with cooling time. The staggered impinging jet cooling was actually activated when the surface temperature reached to a constant at  $900^{\circ}\text{C}$ . This contour shows that mid-peak temperature exists between two adjacent jets, i.e., half of the jet-to-jet spacing of staggered array. The mid-peak temperature was not clearly seen at smaller jet-to-jet spacing ( $S/D = 3$  and  $4$ ), but this was firmly observed at larger jet-to-jet spacing ( $S/D = 5, 6, 8$  and  $10$ ).

As the jet-to-jet spacing becomes greater than  $S/D = 5$ , the mid-peak temperature are more prevailed over half of the jet-to-jet spacing of staggered array. This is highly caused by the hexagonal shape radial flow interaction between the central jet and the surrounding jets as shown in flow visualization of Fig. 5. Actually this radial flow interaction forms a hexagonal shape of water flow stay, so the cooling rate becomes to decrease in the presence of resident water at this area.

Fig. 7 shows time-resolved temperature distribution of the test block through thickness direction at  $S/D = 4$  during staggered array jet cooling.

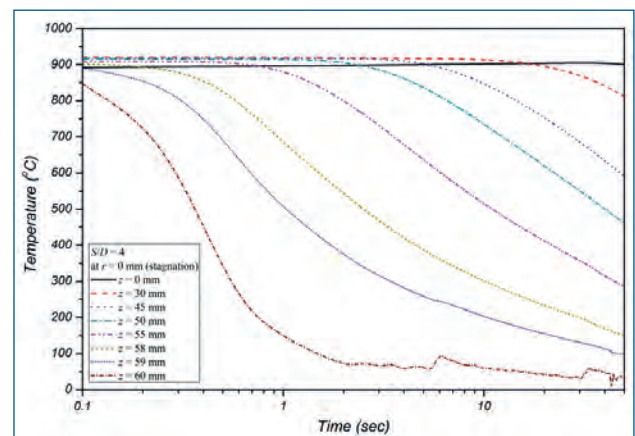
It is seen that the temperature decreases similarly for No. 7 and No. 8 thermocouples which locations are close to the surface. No. 2, 3, 4, 5, and 6 thermocouples exhibit monotonically decreases in temperature through water cooling experiments. The most rapid surface temperature drop occurs at the top surface on which the staggered array jets impinge. As shown in Fig. 7, the surface temperature is quickly decreased below  $100^{\circ}\text{C}$  at approximately 1 second after water jet cooling. This might be characterized by very quick termination of a transition boiling followed by appearance of consistent nucleate boiling as the water impinging jet directly contacts the heated surface.

Fig. 8 shows the difference between the measured and calculated temperature below 1 mm from the top surface at the stagnation point of the central jet ( $r = 0$ ). Symbols represent the measured temperature data inside the test block and lines mean the calculated temperature by 2 dimensional inverse heat conduction formulations which are described before. The difference between the measured and calculated temperature is seen to be less than about 2%. It was observed that the measured temperature is nearly identical to the calculated one. The good agreement between the measured temperature and the calculated value in Fig. 8 indicates that the 2 dimensional inverse heat conduction formulation used in this study predicts quite well the variation in temperature. Fig. 9 shows the local heat flux curves along the radial direction from the stagnation point of the central jet ( $r = 0$ ) to the position of surrounding jet ( $r = 12$ ) at  $S/D = 4$ . The local heat flux curve of stagnation point exhibits the highest values in heat flux curve, and further faster change



**Fig. 6 - Surface temperature contours with change of  $S/D$ .**

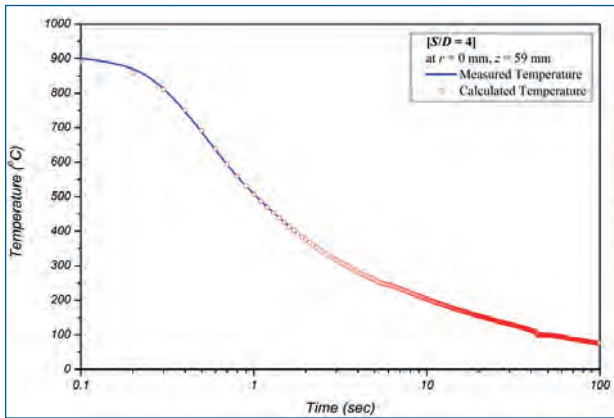
*Fig. 6 - Profili della temperatura superficiale al variare di  $S/D$*



**Fig. 7 - Time-resolved temperature distribution of the test block through thickness.**

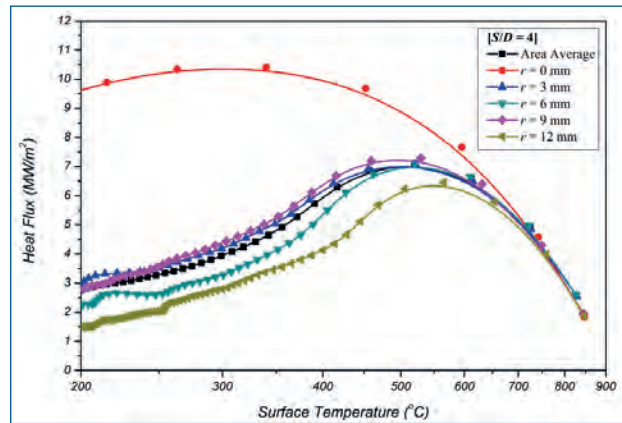
*Fig. 7 - Distribuzione della temperatura nel blocco di prova per diversi affondamenti.*

from transition boiling to nucleate boiling occurs at few seconds after water jet cooling. As the radial interaction between the central jet and the surrounding jets occurs at the location of  $r = 6$ , the local heat flux is correspondingly decreased than that of other positions. The lower heat transfer rate at the location in which the radial interaction between the central jet and the surrounding jets exists



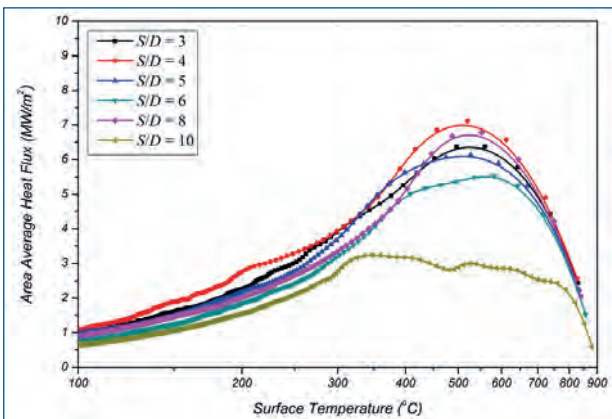
**Fig. 8 - Comparison between the measured and calculated temperature. (1 mm below the top surface)**

Fig. 8 - Confronto fra temperatura misurata e temperatura calcolata. (1 mm sotto la superficie superiore)



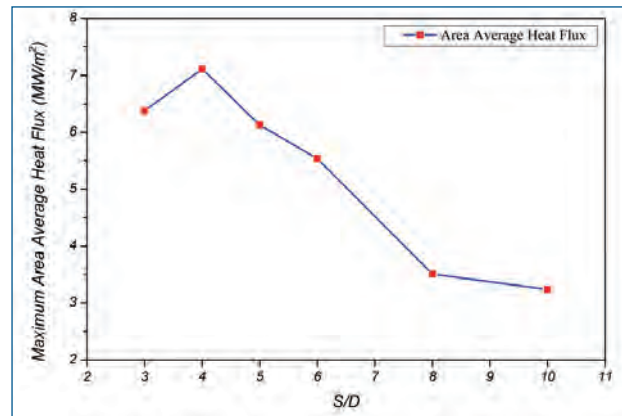
**Fig. 9 - Local heat flux curve along the radial direction at  $S/D = 4$ .**

Fig. 9 - Curva del flusso di calore locale lungo la direzione radiale per  $S/D = 4$ .



**Fig. 10 - Area-average heat flux curve along the different staggered array jet.**

Fig. 10 - Curva del flusso di calore media per area per le diverse configurazioni dei getti sfalsati.



**Fig. 11 Maximum area-average heat flux for tested all staggered array jets.**

Fig. 11 - Massimo flusso di calore medio per area per tutte le diverse configurazioni di getti sfalsati in prova.

implies that the mid-peak temperature occurs at this point as described in Fig. 6.

The area-averaged heat flux curves for the six staggered array of  $S/D = 3, 4, 5, 6, 8$  and  $10$  are shown in Fig. 10. The maximum area-averaged heat flux of this experiment is observed to exist within  $470 \sim 600^\circ\text{C}$ , which is nearly identical to that of a jet impingement boiling [8]. It is seen that the area-averaged heat flux curves do not exhibit any significant pattern in the boiling curve, only except for  $S/D = 10$ .

However, the effects of staggered array jet on maximum area-averaged heat flux seem to be significant, which would be expected as shown in Fig. 11. The maximum value exhibits at  $S/D = 4$ , after then decreases with increasing the jet-to-jet spacing. The maximum area-averaged heat flux value of  $S/D = 4$  is much 2.2 times greater than that

of  $S/D = 10$ . The two possible reason that the maximum area-averaged heat flux occurs at  $S/D = 4$  might be explained. One is based on the flow visualization results as shown in Fig. 5. In case of staggered array, the radial flow issuing from adjacent nozzles interacts influencing area-averaged heat transfer. The other is highly attributed to the existence of a superimposed merging flow within area of half of jet-to-jet spacing which may increase a turbulent intensity between the central jet and the surrounding jets.

## CONCLUSION

An experimental technique using high-temperature heat flux gauge has been used to examine the effects of staggered array jets on water cooling characteristics. This experimental method provided a great advantage of measurement which can be explained by re-use of test

block assembly and simple setup using a high-temperature heat flux gauge, which is compared to conventional steel plate cooling experiments. The flow visualization shows that the radial flow issuing from adjacent nozzles interacts influencing area-averaged heat transfer. The good agreement between the measured temperature and the calculated value indicates that the 2 dimensional inverse heat conduction formulation used in this study predicts quite well the variation in temperature. The maximum area-averaged heat flux value of  $S/D = 4$  is much 2.2 times greater than that of  $S/D = 10$ . The optimized maximum area-averaged heat flux exhibits at  $S/D = 4$ , which can be explained by the radial flow interactions and higher turbulent intensity formed in a superimposed merging flow.

## ACKNOWLEDGEMENT

This work was supported by Energy Efficiency & Resources of the Korea Institute of Energy Technology Evaluation and Planning (KETEP) grant funded by the Korea Government, Ministry of Knowledge Economy (20112010100080).

## REFERENCES

- 1) S.-J. CHEN and A.A. TSENG, *Int. J. Heat Fluid Flow*, 13, (1992), p. 358.
- 2) D.H. WOLF, F.P. INCROPERA, and R. VISKANTA, *Advances in Heat Transfer*, 23, (1993), p. 1.
- 3) Y. PAN and B.W. WEBB, *ASME J. Heat Transfer*, 117, (1995), p. 878.
- 4) J. LEE, *ISIJ International*, 49, (2009), p. 1920.
- 5) S. TWOMEY, *J. Franklin Inst.* 279, (1965), p. 95.
- 6) J.V. BECK, B. BLACKWELL, and C.R. ST. CLAIR, Jr., *Inverse Heat Conduction: Ill-posed Problems*, A Wiley-Interscience, New York (1985).
- 7) G.H. KWON, S.J. KIM, and J. LEE, *Proc. 2012 KSME Fall Conference*, Changwon, Korea (2012).
- 8) N. KARWA, L. SCHMIDT, and P. STEPHEN, *Int. J. Heat Mass Transfer*, 55, (2012), p. 3677.

## Effetto dell'utilizzo di getti sfalsati sulle caratteristiche di raffreddamento dovuto all'impatto dei getti d'acqua su una lastra di acciaio calda

**Parole chiave:** Laminazione - Processi

I getti d'acqua sono ampiamente utilizzati per il raffreddamento delle lamiere di acciaio calde nei processi di fabbricazione. Gli effetti dell'impiego di file di getti sfalsati nei sistemi di raffreddamento a getto d'acqua sono stati studiati con un numero di Reynolds fisso di 35.000 e con una distanza fra ugello e superficie della lamiera di 100 mm. I tempi e la risoluzione spaziale del flusso di calore sono stati misurati sperimentalmente con diverse configurazioni geometriche di disposizioni sfalsate dei getti che sono contrassegnate rispettivamente come 3D, 4D, 5D, 6D, 8D e 10D. Il flusso di calore è stato misurato mediante una nuova tecnica sperimentale che ha la funzione di rilevazione del flusso termico ad alta temperatura. La visualizzazione qualitativa del flusso ha mostrato un comportamento complesso legato alla configurazione sfalsata dei getti, che presenta una interazione radiale del flusso originata dagli ugelli adiacenti. I risultati dimostrano che il massimo flusso di calore medio per area è stato osservato a  $S/D = 4$ . Ciò è stato causato dall'interazione radiale tra getti adiacenti che influenza il trasferimento di calore di ebollizione sulla lamiera calda. In questo studio le curve di flusso di calore misurate vengono anche utilizzate per la creazione di dati di riferimento per la progettazione di un nuovo tipo di impianto di raffreddamento accelerato per laminatoio.